Characterization of the Role of the N-Loop of MIP-1β in CCR5 Binding[†]

Antoine Bondue,[‡] Shu-chuan Jao,[§] Cédric Blanpain,[‡] Marc Parmentier,[‡] and Patricia J. LiWang*[,§]

IRIBHN, Université Libre de Bruxelles, Campus Erasme, 808 route de Lennik, B-1070 Bruxelles, Belgium, and Department of Biochemistry and Biophysics, Texas A&M University, TAMU 2128, College Station, Texas 77843-2128

Received May 7, 2002; Revised Manuscript Received September 3, 2002

ABSTRACT: MIP-1β is a CC-chemokine that plays a role in inflammation and host defense mechanisms by interacting with its specific receptor CCR5. CCR5 is a major coreceptor for macrophage-tropic human immunodeficiency virus (HIV), and as a consequence, MIP-1β can inhibit HIV entry. It is therefore of interest to understand how MIP-1β and other CCR5 ligands bind to their receptor, as such understanding could lead to the rational design of more efficient HIV entry blockers. We have previously demonstrated the importance of Phe13, and of basic residues of the 40's loop, in mediating high-affinity binding of MIP-1β to CCR5. We have now investigated further the relative contribution of other MIP-1β residues in the interaction of the chemokine with CCR5, by studying the functional consequences of point mutations within the N-loop and the 3_{10} turn of MIP-1β, affecting the charge, size, and H-bonding properties of the side chains. Our data suggest that, in addition to Phe13, three amino acids of the N-loop and 3_{10} turn (Arg18, Lys19, and Arg22) interact with CCR5 through their positive charge. We also found that Pro21 contributes to the CCR5 binding properties of MIP-1β. Moreover, NMR spectroscopy has revealed that the presence of Tyr at position 15 is necessary for the proper folding of the chemokine. Our results therefore demonstrate that the binding determinants of MIP-1β consist of residues arranged on one surface of the protein, including most of the basic residues in MIP-1β, as well as two key hydrophobic groups. The good correlation observed between the potency of the mutants in a functional assay and their binding affinity strongly argues that basic residues Arg18, Lys19, and Arg22 of MIP-1β are essential for its CCR5 binding properties, without a primary effect on CCR5 activation.

Chemokines are small secreted proteins involved in the recruitment and activation of leukocytes during the inflammatory response and in the homing of the various immune cell populations. By regulating leukocyte trafficking, they play a central role in the development of inflammatory diseases, including rheumatoid arthritis, atherosclerosis, and multiple sclerosis (*1*). For these reasons, chemokine receptors are considered to be attractive as candidates for therapeutic intervention. Chemokines and chemokine receptors also play a central role in HIV[1] pathogenesis: the chemokine receptors CCR5 and CXCR4 are the main coreceptors allowing HIV entry, and the chemokine MIP-1β, among others, is able to block cellular entry of macrophage-tropic primary HIV isolates, which are responsible for disease transmission. Therefore, the understanding of the complex structure−function relationships of CCR5 and its ligands may help in the rational design of new and effective drugs.

The chemokine superfamily includes more than 40 proteins subdivided into two major (CC and CXC) and two minor (C and CX_3C) subfamilies according to the relative position of their first two conserved cysteines. All chemokines share a conserved monomeric fold composed of a disordered N-terminus, a relatively long first loop (the so-called "N-loop"), three antiparallel β-strands separated by short loops, and a C-terminal α-helix. As for all CC-chemokines, the first two cysteines of MIP-1β are contiguous, separating the N-terminal domain from the N-loop that spans residues 13−19 (Figure 1A). The N-loop is followed by the "3_{10} turn" that includes residues 20−24, and precedes the first β-strand.

The functional analysis of different chemokines has led to the general conclusion that the N-terminal domain of these proteins is necessary for triggering receptor signaling, while the core domain of the molecules contains the motifs responsible for their tight binding to the receptors (*2*−*4*). Experimental evidence that directly supports the role of the N-loop in receptor binding has been reported for other CC-chemokines, such as RANTES, MCP-1, and recently eotaxin

[†] Funding was provided by the National Science Foundation (Grant MCB 9996369) and by the Robert Welch Foundation. M.P. was supported by the Actions de Recherche Concertées of the Communauté Française de Belgique, the French Agence Nationale de Recherche sur le SIDA, and the BIOMED and BIOTECH programs of the European Community (Grants BIO4-CT98-0543 and BMH4-CT98-2343). C.B. is Aspirant of the Belgian Fonds National de la Recherche Scientifique.

* To whom correspondence should be addressed: Department of Biochemistry and Biophysics, Texas A&M University, TAMU 2128, College Station, TX 77843-2128. E-mail: pliwang@tamu.edu. Telephone: (979) 845-5616. Fax: (979) 845-9274.

[‡] Université Libre de Bruxelles.

[§] Texas A&M University.

[1] Abbreviations: CCR, CC chemokine receptor; CHO, Chinese hamster ovary; DSS, 4,4-dimethyl-4-silapentane-1-sulfonate; DMEM, Dulbecco's modified Eagle's medium; HIV, human immunodeficiency virus; HSQC, heteronuclear single-quantum coherence; FACS, fluorescence-activated cell sorting; BSA, bovine serum albumin; MCP-1, monocyte chemotactic protein-1; MIP-1, macrophage inflammatory protein-1; NMR, nuclear magnetic resonance; RANTES, regulated upon activation, normal T cells expressed and secreted; SDF-1, stromal cell-derived factor-1; GAG, glycosaminoglycan; TFA, trifluoroacetic acid; SEM, standard error of the mean.

10.1021/bi026087d CCC: $22.00
Published on Web 10/26/2002

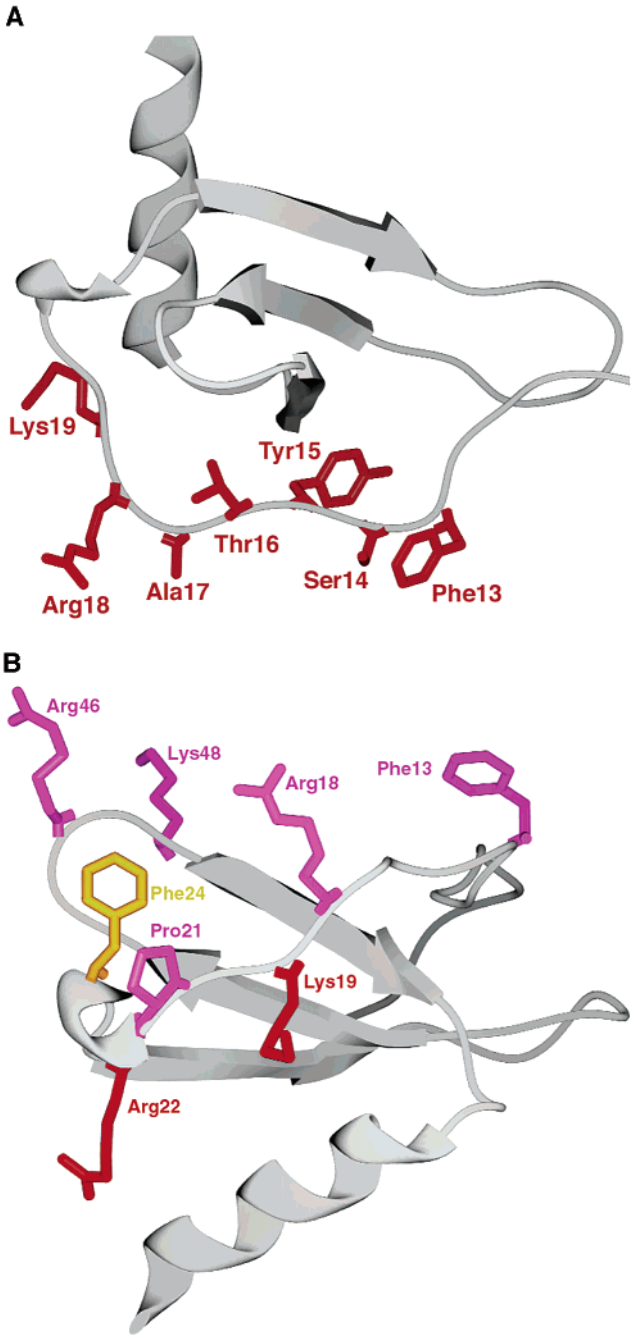

FIGURE 1: (A) Three-dimensional structure of MIP-1β, as derived from NMR spectroscopy (*15*), showing the residues of the N-loop. (B) Spatial orientation of residue side chains involved in MIP-1β binding to CCR5; residues in purple and in red have been shown here or in a previous study (*9*) to be important to CCR5 binding. The residue in yellow (Phe24) was postulated by its orientation to be involved in CCR5 binding, but studies of Phe24Ala showed wild-type function.

(*4*−*7*). Recently, we have demonstrated the major role of the aromatic side chain of MIP-1β's Phe13 in CCR5 binding (*3*, *8*), but the role of other residues of MIP-1β's N-loop is largely unexplored. Also, the N-loop is not the only region involved in chemokine receptor binding, and we have shown recently that R46 and K48, residues located in the so-called "40's loop", constitute an important determinant involved in CCR5 binding (*9*).

Unlike other CCR5-binding proteins, MIP-1β is unique in having little or no function on other receptors, making the understanding of the structural features responsible for CCR5 binding valuable in the design of specific, CCR5-targeted therapeutics. To more fully determine the CCR5 binding determinants of MIP-1β, and to precisely delineate their role in receptor activation, we have generated MIP-1β variants bearing mutated residues within the N-loop and the 3_{10} turn, and changed the charge, size, or H-bonding properties of these side chains. Our study confirms the role of Phe13 and points toward the contribution of three basic residues (R18, K19, and K22) to the CCR5 binding site of MIP-1β. We also found that P21, located within the 3_{10} turn, contributes to CCR5 binding. Moreover, we show that, despite their obvious role in determining the affinity of the chemokine for CCR5, none of these residues is directly involved in the activation of the receptor.

EXPERIMENTAL PROCEDURES

Production and Purification of MIP-1β Variants. Mutations in MIP-1β were produced using the Quikchange procedure (Stratagene, La Jolla, CA) in a variant of pET32-Xa/LIC (Novagen, Madison, WI). All mutations were confirmed through DNA sequencing. These MIP-1β variants were produced in bacteria and purified as previously described (*3*). Briefly, the proteins were expressed in BL21-(DE3) cells transformed with a variant of the pET32LICXa vector in which the thioredoxin fusion partner has been removed, leaving a smaller fusion tag. The cells were then resuspended in 500 mM NaCl, 20 mM Tris (pH 8), and 10 mM benzamidine and French pressed twice at 16 000 psi. Under these conditions, most MIP-1β variants are found in the insoluble portion of the suspension. After centrifugation for 1 h at 12000*g*, the pellet was resuspended in 10 mL of 5−7 M guanidinium, 50 mM Tris (pH 8), 50 mM NaCl, 2 mM EDTA, and 10 mM β-mercaptoethanol. The solution was centrifuged briefly to remove insoluble matter and then was refolded by adding it slowly to 100 mL of 50 mM Tris (pH 8), 50 mM NaCl, 2 mM EDTA, and 5 mM β-mercaptoethanol. The diluted protein solution was allowed to remain at room temperature for 2 h, and then was dialyzed at 4 °C in 20 mM Tris (pH 8) to remove guanidine. After dialysis, precipitated matter was removed by centrifugation, trifluoroacetic acid was added to 0.1%, and the solution was purified on a C4 reversed phase chromatography column, and lyophilized. To remove the fusion tag, the protein powder was solubilized in 20 mM sodium phosphate (pH 2.5) the volume was increased to ~40 mL in 20 mM Tris (pH 8), 50 mM NaCl, and 2 mM $CaCl_2$. Factor Xa (Novagen) was used to effect cleavage, and the mature MIP-1β variants were purified a final time over a C4 reversed phase column. Samples were lyophilized, and for NMR, the dry powder was dissolved in a 20 mM sodium phosphate buffer (pH 2.5) containing 0.02% NaN_3 (Sigma).

NMR Spectroscopy. NMR spectra were measured at 25 °C on a Varian Inova 500 or Varian Inova 600 spectrometer, equipped with an xyz gradient penta probe (500) or an xyz gradient triple-resonance probe (600). ^{15}N-HSQC spectra were measured with 512* points in the ^{1}H dimension, and 128* points in the ^{15}N dimension. Typically, a 6000 Hz sweep width (500 MHz) or a 8000 Hz sweep width (600 MHz) was used for ^{1}H, while a 1600 Hz sweep width was used for ^{15}N. The spectra were referenced relative to DSS.

CCR5-Expressing Cell Lines. A CHO-K1 cell line expressing an apoaequorin variant targeted to mitochondria (*10*) under control of the SRα promoter (*11*), and selected on the basis of its luminescent response to ionomycin A (100 nM) and ATP (10 μM), has been described previously (*12*). A construct encoding wild-type CCR5 in the pEFIN3 bicistronic vector was further transfected using Fugene 6 (Boehringer Mannheim) in this apoaequorin-expressing cell line. Following selection with 400 μg/mL G418 (Life Technologies) for 14 days, the population of mixed cell clones was used in binding and functional studies. CHO-K1 cells were cultured in HAM's F12 medium supplemented with 10% fetal calf serum (Life Technologies), 100 units/mL penicillin, and 100 μg/mL streptomycin (Life Technologies).

Binding Assays. CHO-K1 cells expressing wild-type CCR5 were collected from plates with Ca^{2+} and Mg^{2+}-free PBS supplemented with 5 mM EDTA, gently pelleted for 2 min at 1000*g*, and resuspended in binding buffer [50 mM Hepes (pH 7.4), 1 mM $CaCl_2$, 5 mM $MgCl_2$, and 0.5% BSA]. Competition binding assays were performed in Minisorb tubes (Nunc), using 0.08 nM [^{125}I]MIP-1β (Amersham-Pharmacia Biotech, 2000 Ci/mmol) as a tracer, variable concentrations of MIP-1β or its mutants, and 40 000 cells in a final volume of 0.1 mL. The level of total binding was measured in the absence of competitor, and the level of nonspecific binding was measured with a 100-fold excess of unlabeled ligand. Samples were incubated for 90 min at 27 °C, and then the bound tracer was separated by filtration through GF/B filters presoaked in 1% BSA. Filters were counted in a β-scintillation counter. Binding parameters were determined with Prism software (GraphPad Software) using nonlinear regression applied to a one-site competition model.

Functional Assays. The functional response of CCR5-expressing cells to chemokines was analyzed by measuring the luminescence of aequorin as described previously (*12*−*14*). Cells were collected from plates with Ca^{2+} and Mg^{2+}-free DMEM supplemented with 5 mM EDTA, pelleted for 2 min at 1000*g*, resuspended in DMEM at a density of 5×10^6 cells/mL, and incubated for 2 h in the dark in the presence of 5 μM coelenterazine H (Molecular Probes). Cells were diluted 5-fold before being used. Agonists in 50 μL of DMEM were added to 50 μL of a cell suspension (50 000 cells), and luminescence was measured for 30 s in a Berthold luminometer.

RESULTS

To assess the contribution of the size, charge, and H-bonding properties of each amino acid side chain within the N-loop and 3_{10} turn of MIP-1β, we engineered the following point mutants of the chemokine: S14A, S14V, S14T, Y15A, T16A, A17S, A17V, R18A, R18K, R18Q, R18E, K19E, K19A, and R22E. Taking into account the three-dimensional structure of MIP-1β (*15*), we considered that residues pointing in the same direction as Arg46, Lys48, and Phe13, three residues involved in CCR5 binding (*3*, *9*), might contribute to binding as well. We therefore mutated P21 and F24 also, which fulfill this criterion (Figure 1B). These MIP-1β mutants were expressed in BL21(DE3) cells, refolded, and purified as described above. After characterization of their tertiary structure by NMR spectroscopy, all mutants were studied for their ability to bind CCR5, and to trigger calcium release in CCR5-expressing cells.

Role of the N-Loop of MIP-1β (Residues 13−*19).* The analysis of mutants by NMR spectroscopy revealed that Tyr15 plays an important role in maintaining the tertiary structure of MIP-1β, as substitution with an alanine resulted in an unfolded protein refractory to all refolding attempts (data not shown). For this reason, this variant was not tested further in binding and functional assays.

Replacing Ser14 with an alanine, a valine, or a threonine resulted in a shift in the position of the Phe13 resonance in ^{15}N-HSQC spectra of these variants, although there appears to be little further alteration of the MIP-1β structure (Figure 2B). Two of these variants, S14A and S14V, additionally showed changes in the Ser33 resonance, which is across the dimer interface from Ser14. The replacement of Thr16 with an alanine resulted in more peak modifications than for any other folded N-loop mutant except Phe13, including changes to adjacent residues T15 and Ala17, as well as chemical shift changes in more distal residues such as Phe13, Val25, and Ala52 (Figure 2C). Substitution of Ala17, Arg18, or Lys19 did not alter the structure of the molecule, as evidenced by very little chemical shift change compared to the wild-type protein (Figure 2D and data not shown).

As previously shown, Phe13 appeared as a major site involved in the binding of MIP-1β to CCR5 (Figure 3A); replacing Phe13 with alanine resulted in a purely monomeric protein with a dramatic loss of affinity for CCR5. Table 1 summarizes the IC_{50} values obtained for each mutant in a CCR5 binding assay, using wild-type MIP-1β as a tracer. Despite the change in the Phe13 position observed in NMR spectroscopy following substitutions of Ser14, lengthening the side chain (S14T) or removing the H-bonding capability (S14V) of this amino acid did not affect the ability of the molecule to bind CCR5 (Figure 3A and Table 1). The substitution of Thr16 with Ala, and of Ala17 with Val or Ser, did not affect the CCR5 binding properties of MIP-1β (Figure 3A and Table 1).

The replacement of Arg18 with alanine resulted in a moderate loss of affinity for CCR5 (mean IC_{50} of 0.86 nM compared to a value of 0.37 nM for the wild-type protein) (Figure 3A and Table 1). Substitution of Arg18 with a glutamine resulted in a similar reduction in affinity (IC_{50} of 1.15 nM). This effect was more dramatic when the positive charge of the side chain was replaced with the negative charge of a glutamic acid (mean IC_{50} of 7.76 nM). On the other hand, the conservation of the positive charge in the R18K mutant allowed it to keep an affinity similar to that of wild-type MIP-1β (mean IC_{50} of 0.45 nM). These results strongly suggested that residue 18 interacts with CCR5 through the positive charge of its side chain.

Similarly, changing the positive charge of Lys19 to a negatively charged glutamic acid resulted in a significant loss of affinity for CCR5 (IC_{50} of 3.25 nM) (Figure 3A and Table 1). A milder reduction in affinity was observed when Lys19 was mutated to alanine (IC_{50} of 0.78 nM).

To investigate the role of MIP-1β N-loop residues in CCR5 activation, we tested the ability of the mutants to trigger intracellular calcium release in a cell line coexpressing CCR5 and apoaequorin, as previously described (*12*). Mutations of amino acids 14, 16, and 17, which did not impair the affinity for CCR5 in a binding assay, did not affect the functional response of CCR5 to these mutant chemokines

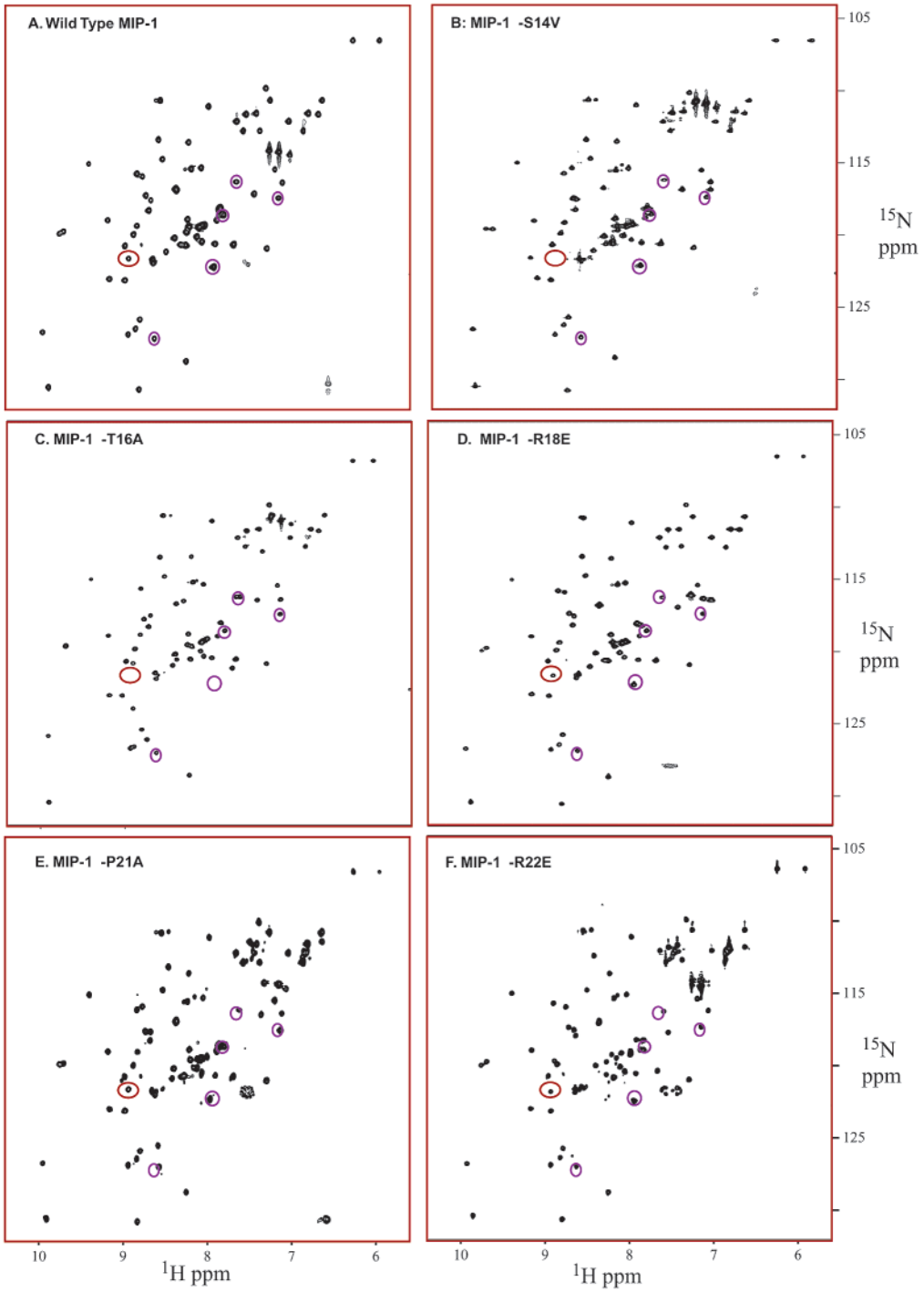

FIGURE 2: HSQC spectra of wild-type MIP-1β (A) and mutants S14V (B), T16A (C), R18E (D), P21A (E), and R22E (F) in 20 mM sodium phosphate buffer. The circles highlight the positions of the peaks corresponding to residues shown to be important in CCR5 binding in wild-type MIP-1β, including Phe13 (red circle) and Arg18, Lys19, Arg22, Arg46, and Lys48 (purple circles). Empty circles indicate that the mutation has resulted in an alteration in the environment of the residue, leading to a peak shift.

(Figure 3B and Table 1). In addition, the reduction of potency for the Arg18 and Lys19 mutants observed in the functional assay was well correlated to the reduction in affinity observed in the binding assay, demonstrating that these residues are primarily involved in CCR5 binding, but not directly in its activation (Figure 3B and Table 1).

Role of the 3_{10} Turn of MIP-1β (Residues 20−24). Structurally, mutation of proline 21 to alanine affected amino acids 18−25 in the ^{15}N-HSQC spectrum (Figure 2E), indicating local changes in the structure of the protein with this mutation. The NMR spectrum of the R22E mutant showed no major change in the structure of the protein, even though minor changes in the chemical shift of adjacent residues as well as of more distal positions were observed (Figure 2F). The mutation F24A shows essentially no chemical shift changes in residues 11−18, with some peak shifting observed in residues close in sequence to Phe24. There are also significant shifts in resonances 46−50, likely due to the close contact of these amino acids with Phe24 in the structure of the protein (data not shown).

Functionally, a severe decrease in CCR5 binding affinity was observed when the positive charge of Arg22 was

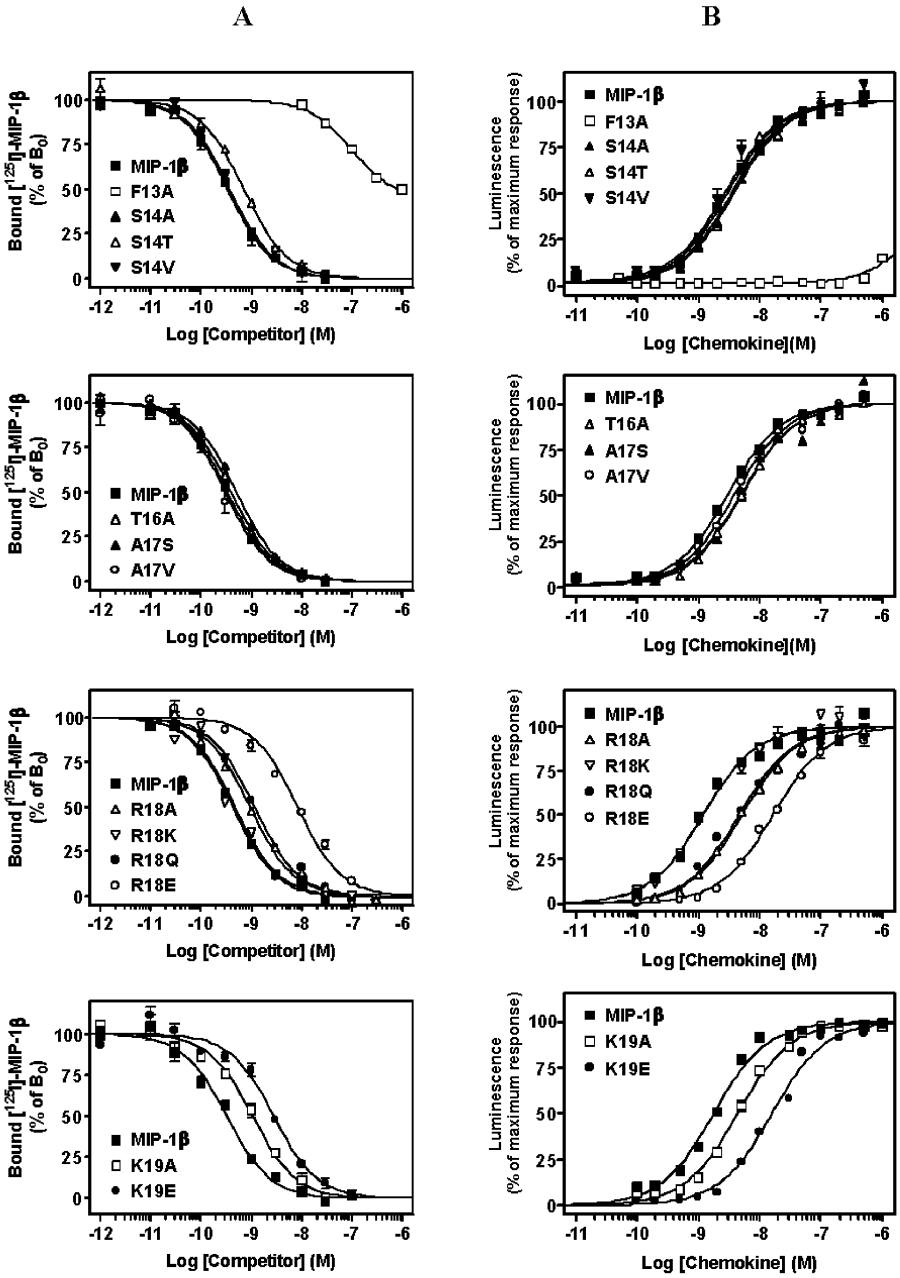

FIGURE 3: Characterization of the binding and functional properties of N-loop mutants of MIP-1β. (A) Competition binding curves were determined on a CHO-K1 cell line expressing CCR5, using 0.08 nM [^{125}I]MIP-1β as a tracer. The data were normalized for nonspecific binding (0%) and maximal specific binding in the absence of a competitor (100%). The results were analyzed with GraphPad PRISM software using a single-site model. All points were run in triplicate (error bars represent the standard error of the mean), and the presented data set is representative of two independent experiments. (B) Functional dose−response curves obtained on CHO-K1 cells coexpressing apoaequorin and CCR5. The luminescent signal resulting from the intracellular calcium release induced by MIP-1β mutants was recorded in a luminometer. The results were analyzed by nonlinear regression using GraphPad PRISM software. The data were normalized to basal luminescence (0%) and the maximal luminescence signal resulting from ATP stimulation (100%). All points were run in triplicate (error bars represent the standard error of the mean). The displayed curves represent a typical experiment of two performed independently.

replaced with a negative one (Figure 4A and Table 1). Indeed, the R22E mutant displayed an IC_{50} of 5.99 nM, as compared to a value of 0.37 nM for wild-type MIP-1β. The replacement of Pro21 with alanine resulted in a 4-fold decrease in CCR5 binding affinity (IC_{50} of 1.42 nM) (Figure 4A and Table 1), whereas no significant change was observed when Phe24 was replaced with alanine (Figure 4A and Table 1). As was found for the MIP-1β N-loop mutants, the ability of 3_{10} turn mutants to activate CCR5 in a functional assay was well correlated with the affinity parameters determined in the binding assay (Figure 4B and Table 1).

DISCUSSION

A number of studies have identified residues in chemokines involved in their interaction with receptors, but the molecular details of how chemokines bind to their receptors and trigger the conformational change resulting in their activation remains largely unknown. A two-site model has been proposed (*2*, *16*), defining grossly the chemokine−chemokine receptor interaction, and is generally consistent with most experimental data. This model postulates that the core domain of the chemokine establishes first a high-affinity interaction with the extracellular domains of the receptor,

Table 1: Binding and Functional Parameters Characterizing the Interaction of MIP-1β Analogues with CCR5[a]

	$pIC_{50} \pm SEM$	$pEC_{50} \pm SEM$
MIP-1β	9.43 ± 0.08	8.64 ± 0.08
S14A	9.46 ± 0.04[b]	8.28 ± 0.14[b]
S14V	9.21 ± 0.15[b]	8.50 ± 0.05[b]
S14T	9.20 ± 0.06[b]	8.38 ± 0.08[b]
T16A	9.34 ± 0.15[b]	8.32 ± 0.02[b]
A17S	9.38 ± 0.09[b]	8.29 ± 0.00[b]
A17V	9.35 ± 0.13[b]	8.35 ± 0.07[b]
R18A	9.06 ± 0.11[c]	7.99 ± 0.15[d]
R18K	9.35 ± 0.02[b]	8.35 ± 0.29[b]
R18Q	8.94 ± 0.00[c]	8.05 ± 0.14[d]
R18E	8.11 ± 0.11[e]	7.50 ± 0.23[e]
K19E	8.49 ± 0.11[e]	7.89 ± 0.14[e]
K19A	9.11 ± 0.11[b]	8.36 ± 0.11[b]
P21A	8.85 ± 0.09[d]	8.00 ± 0.11[d]
R22E	8.22 ± 0.13[e]	7.83 ± 0.02[d]
F24A	9.37 ± 0.13[b]	8.46 ± 0.08[b]

[a] The pIC_{50} value for each mutant was obtained in a competitive binding assay, using a CCR5-expressing CHO-K1 cell line, and [^{125}I]MIP-1β as a tracer. The pEC_{50} values (protein concentration generating 50% of the maximal response) were obtained in a functional assay in which the luminescence of CCR5- and apoaequorin-expressing cells is monitored in response to the stimulation by the MIP-1β mutants. The values represent the mean $\pm$ SEM resulting from at least two independent experiments. The statistical significance as compared to that of wild-type MIP-1β was calculated with the Student's *t* test. [b] Not significant. [c] $p < 0.05$. [d] $p < 0.01$. [e] $p < 0.001$.

followed by an interaction between the N-terminal domain of the chemokine and the transmembrane segments of the receptor, resulting in its activation. In an effort to evaluate the role of the N-loop and the 3_{10} turn of MIP-1β in CCR5 binding and activation, we generated mutants affecting the charge, size, and H-bonding capabilities of the amino acid side chains of many residues in this region, and tested them in binding and functional assays. For each of the mutants, gross modifications in their tertiary structure were first assessed by NMR. Mutation at Tyr15 was unique in having a detrimental effect on the structure of MIP-1β, as the Y15A variant resisted attempts to refold the protein. Therefore, mutations at this position were not studied further.

Significance of the N-Loop and 3_{10} Turn in MIP-1β Binding to CCR5. To support the importance of the N-loop of MIP-1β in receptor binding, we have previously demonstrated the critical role of Phe13 in CCR5 binding, and the involvement of the aromatic nature of the residue side chain by extensive mutations at this position (*3*, *8*). An aromatic residue at the same position has been shown to play a central role in the binding of other CC-chemokines to their respective receptors (*4*−*6*). This aromatic residue is not shared by CXC-chemokines and may therefore represent a common binding site, specific for CC-chemokines, that might contribute to the promiscuous binding of these ligands to CC-chemokine receptors. Despite the major role of Phe13 in MIP-1β binding to CCR5, alterations in the local environment of this residue did not appear to be detrimental to the binding properties of the chemokine. Indeed, mutations of Ser14 induced a significant change in the chemical shift for the backbone H^N of the critical adjoining F13, as demonstrated by NMR, but this local change in MIP-1β structure did not affect the ability of the chemokine to bind and activate CCR5.

Besides Phe13, basic residues of the N-loop also appeared to be critical for MIP-1β binding to CCR5. We have previously shown that the charged residues R46 an K48, located in the 40's loop of MIP-1β, play an important role in binding (*9*). Here, we show that the three basic residues (R18, K19, and R22), located in the N-loop and 3_{10} turn, are important as well. Moreover, the substitution of these residues with various amino acids indicated that the interaction with CCR5 likely involves their positively charged side chain. Thus, two clusters of basic residues appear so far to be involved in the contact between MIP-1β and CCR5: one in the 40's loop (R46 and K48) and the other in the N-loop and 3_{10} turn (R18, K19, and R22). The role of basic residues in other closely related CC-chemokines has also been investigated. From these results, it appears that some conserved basic residues contribute to receptor binding in most analyzed chemokines, whereas other basic residues appear to be specific for a given chemokine (*4*−*7*, *9*, *17*−*19*). It seems likely that the conserved basic residues would interact with conserved negatively charged residues within the receptors. Candidate regions for such interactions might include the clusters of acidic residues, consistently present in the amino-terminal domain of CC-chemokine receptors (*12*). Some of the tyrosines of these motifs have been shown to be sulfated, increasing the overall negative charge of this amino-terminal domain (*20*). When the role of the aromatic residue Phe13, located in the N-loop, is considered, the results presented here suggest that the binding surface of MIP-1β can be seen as a hydrophobic pocket surrounded by multiple charged basic residues (Figure 1B).

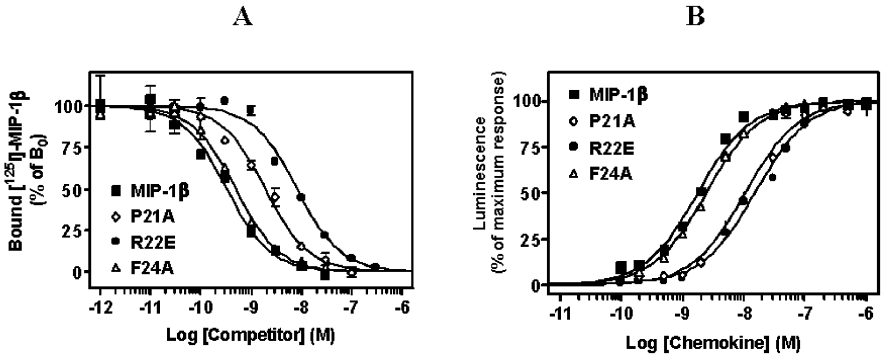

FIGURE 4: Characterization of the binding and functional properties of 3_{10} turn mutants of MIP-1β. (A) Competition binding curves were determined and analyzed as described in the legend of Figure 3. All points were run in duplicate (error bars represent the standard error of the mean), and the presented data set is representative of two independent experiments. (B) Functional dose−response curves were obtained and analyzed as described in the legend of Figure 3. All points were run in duplicate (error bars represent the standard error of the mean). The displayed curves represent a typical experiment of two performed independently.

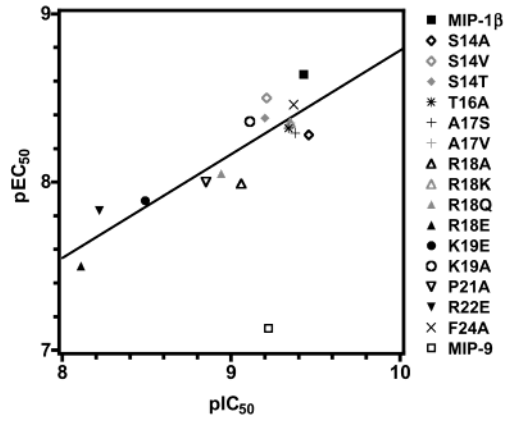

FIGURE 5: Correlation between the pIC_{50} and pEC_{50} values of wild-type MIP-1β and the MIP-1β mutants used in this study. The linear regression indicates a good correlation between the binding and functional parameters ($r^2 = 0.94$). As an example of a mutant for which binding and activation are not correlated, we introduced the parameters obtained for MIP-9, a truncated MIP-1β mutant, that binds but does not activate CCR5 well (*3*).

The mutation of Pro21 resulted in a small decrease in binding affinity. Pro21 might therefore contribute directly to CCR5 binding, or alternatively, the alanine substitution of Pro21 might modify the position of Arg22, and affect binding indirectly. No major change in the structure of this P21A mutant was observed in the NMR spectrum of the molecule, although the chemical shift of several nearby residues, including Arg22 and Lys19, had changed, suggesting a slight structural alteration in support of this latter hypothesis.

Absence of a Role of the N-Loop and the 3_{10} Turn of MIP-1β in CCR5 Activation and Implications for Drug Design. Our results demonstrated the apparent absence of a role of the MIP-1β N-loop in the mechanism of CCR5 activation (Figure 5). This observation therefore supports the current two-site model of chemokine−receptor interaction, in which the core domain of chemokines mediates receptor binding, without contributing much to receptor activation. However, for some chemokines, it has been proposed that residues located outside the N-terminal domain could mediate receptor activation (*7*, *19*, *21*).

These results in conjunction with those of others indicate that a tight binding motif for CCR5 includes an essential aromatic group along with multiple quaternary ammonium groups. In support of this, a recent study that included a series of peptides from RANTES showed that nearly every CCR5-binding or HIV-inhibiting peptide contained a Phe followed within a few amino acids by a positively charged amino acid (*5*). Our binding model is also supported by the effectiveness of the small molecule TAK-779 that functions as an anti-HIV agent by binding CCR5 (*22*). The structure of TAK-779 includes a large aromatic portion separated by several bonds from a quaternary ammonium group, consistent with our model for MIP-1β binding in which positively charged nitrogens, guanidinium (Arg) or ammonium (Lys), support the interaction provided by the essential aromatic Phe. Indeed, our results suggest that the presence of additional quaternary ammonium groups may help the binding capabilities of this or other small molecule inhibitors of CCR5.

In conclusion, it appears from this study and earlier studies that multiple residues of MIP-1β are involved in the constitution of the binding site of CCR5. The combination of an aromatic amino acid (Phe13), and a number of positively charged amino acids (including Arg18, Lys19, Arg22, Arg46, and Lys48), seems to constitute points of tight binding to the receptor. In accordance with the two-site model of chemokine−receptor interaction, none of these residues (all located outside the N-terminal domain) contributes to CCR5 activation. This work delineates important residues involved in CCR5 binding by MIP-1β and has implications for the design of tight-binding therapeutics.

ACKNOWLEDGMENT

We thank Craig Cassidy, Jason Quinlan, Taehun Park, Gwen Knapp, Xin Liu, and Carrie Langlais. The NMR instrumentation in the Biomolecular NMR Laboratory at Texas A&M University was supported by a grant from the National Science Foundation (DBI-9970232) and the Texas A&M University System.

REFERENCES

1. Gerard, C., and Rollins, B. J. (2001) *Nat. Immunol. 2*, 108−115.
2. Clark-Lewis, I., Kim, K. S., Rajarathnam, K., Gong, J. H., Dewald, B., Moser, B., Baggiolini, M., and Sykes, B. D. (1995) *J. Leukocyte Biol. 57*, 703−711.
3. Laurence, J. S., Blanpain, C., Burgner, J. W., Parmentier, M., and LiWang, P. J. (2000) *Biochemistry 39*, 3401−3409.
4. Pakianathan, D. R., Kuta, E. G., Artis, D. R., Skelton, N. J., and Hebert, C. A. (1997) *Biochemistry 36*, 9642−9648.
5. Nardese, V., Longhi, R., Polo, S., Sironi, F., Arcelloni, C., Paroni, R., DeSantis, C., Sarmientos, P., Rizzi, M., Bolognesi, M., Pavone, V., and Lusso, P. (2001) *Nat. Struct. Biol. 8*, 611−615.
6. Hemmerich, S., Paavola, C., Bloom, A., Bhakta, S., Freedman, R., Grunberger, D., Krstenansky, J., Lee, S., McCarley, D., Mulkins, M., Wong, B., Pease, J., Mizoue, L., Mirzadegan, T., Polsky, I., Thompson, K., Handel, T. M., and Jarnagin, K. (1999) *Biochemistry 38*, 13013−13025.
7. Mayer, M. R., and Stone, M. J. (2001) *J. Biol. Chem. 276*, 13911−13916.
8. Kim, S., Jao, S., Laurence, J. S., and LiWang, P. J. (2001) *Biochemistry 40*, 10782−10791.
9. Laurence, J. S., Blanpain, C., De Leener, A., Parmentier, M., and LiWang, P. J. (2001) *Biochemistry 40*, 4990−4999.
10. Takebe, Y., Seiki, M., Fujisawa, J., Hoy, P., Yokota, K., Arai, K., Yoshida, M., and Arai, N. (1988) *Mol. Cell. Biol. 8*, 466−472.
11. Rizzuto, R., Pinton, P., Carrington, W., Fay, F. S., Fogarty, K. E., Lifshitz, L. M., Tuft, R. A., and Pozzan, T. (1998) *Science 280*, 1763−1766.
12. Blanpain, C., Doranz, B. J., Vakili, J., Rucker, J., Govaerts, C., Baik, S. S., Lorthioir, O., Migeotte, I., Libert, F., Baleux, F., Vassart, G., Doms, R. W., and Parmentier, M. (1999) *J. Biol. Chem. 274*, 34719−34727.
13. Stables, J., Green, A., Marshall, F., Fraser, N., Knight, E., Sautel, M., Milligan, G., Lee, M., and Rees, S. (1997) *Anal. Biochem. 252*, 115−126.
14. Blanpain, C., Lee, B., Vakili, J., Doranz, B. J., Govaerts, C., Migeotte, I., Sharron, M., Dupriez, V., Vassart, G., Doms, R. W., and Parmentier, M. (1999) *J. Biol. Chem. 274*, 18902−18908.
15. Lodi, P. J., Garrett, D. S., Kuszewski, J., Tsang, M. L., Weatherbee, J. A., Leonard, W. J., Gronenborn, A. M., and Clore, G. M. (1994) *Science 263*, 1762−1767.
16. Wells, T. N., Power, C. A., Lusti-Narasimhan, M., Hoogewerf, A. J., Cooke, R. M., Chung, C. W., Peitsch, M. C., and Proudfoot, A. E. (1996) *J. Leukocyte Biol. 59*, 53−60.
17. Martin, L., Blanpain, C., Garnier, P., Wittamer, V., Parmentier, M., and Vita, C. (2001) *Biochemistry 40*, 6303−6318.
18. Proudfoot, A. E., Fritchley, S., Borlat, F., Shaw, J. P., Vilbois, F., Zwahlen, C., Trkola, A., Marchant, D., Clapham, P. R., and Wells, T. N. (2001) *J. Biol. Chem. 276*, 10620−10626.

19. Harrison, J. K., Fong, A. M., Swain, P. A., Chen, S., Yu, Y. R., Salafranca, M. N., Greenleaf, W. B., Imai, T., and Patel, D. D. (2001) *J. Biol. Chem. 276*, 21632−21641.
20. Farzan, M., Mirzabekov, T., Kolchinsky, P., Wyatt, R., Cayabyab, M., Gerard, N. P., Gerard, C., Sodroski, J., and Choe, H. (1999) *Cell 96*, 667−676.
21. Blanpain, C., Buser, R., Power, C. A., Edgerton, M., Buchanan, C., Mack, M., Simmons, G., Clapham, P. R., Parmentier, M., and Proudfoot, A. E. (2001) *J. Leukocyte Biol. 69*, 977−985.
22. Baba, M., Nishimura, O., Kanzaki, N., Okamoto, M., Sawada, H., Iizawa, Y., Shiraishi, M., Aramaki, Y., Okonogi, K., Ogawa, Y., Meguro, K., and Fujino, M. (1999) *Proc. Natl. Acad. Sci. U.S.A. 96*, 5698−5703.

BI026087D